Design Considerations of Engraved NRD Guide for Millimeter-Wave Integrated Circuits

Yves Cassivi, Dominic Deslandes, and Ke Wu, *Fellow, IEEE*

***Abstract*—Practical construction of nonradiative dielectric (NRD) guide components such as filter, junction, or hybrid planar NRD-guide circuit is rather uneasy because of the tedious alignment and tolerance requirement of various separate NRD-guide elements. To overcome this hurdle, we present a new scheme called the engraved NRD guide (ENRD). This ENRD guide is an NRD guide whose outline is machined out of a single dielectric block, thereby eliminating the alignment constraint, and allowing a better precision for physical design, realization, and integrity of the overall circuit. Design considerations and procedures of the ENRD guide are studied and discussed in this paper, which suggest the predominance of gap dimension in obtaining a quasi-nonradiative condition with similar propagation properties as a normal NRD guide. It also shows that the amount of dielectric material left in support of the whole structure alignment could greatly affect the leakage level of the guide. An ENRD-guide 90° bend and filter were designed and measured. Investigation of the ENRD-guide filter leads to the characterization of an evanescent LSM_{10} mode in the air gap region between the resonators necessary for reducing its insertion loss.**

***Index Terms*—Electromagnetic coupling, filter, hybrid integration of planar circuits and NRD guide, millimeter-wave technology, nonradiative dielectric waveguide, transmission line.**

I. Introduction

SINCE ITS inception [1], the nonradiative dielectric (NRD) guide has been used in the design of a large number of millimeter-wave integrated circuits and antennas [2]–[5]. In all those applications, particularly in filter design, the practical construction of NRD-guide circuits requires a high accuracy in the alignment of NRD-guide building pieces and blocks. One must find a way, for example, in the case of an air-gap NRD resonator filter, to adequately fix a designated physical layout of the multiple dielectric resonators by using glue or other means relative to the parallel metal plates. This problem is significant at millimeter-wave frequencies at which the precision of alignment should be much better than 50 μm, depending on the dielectric constant of the material used. On the other hand, the commercial applications of NRD-guide technology demand a reliable and repeatable low-cost process for massive fabrication.

A grooved NRD guide was introduced to tackle this problem [6], [7]. In this case, the two metallic plates (only one for the asymmetric geometry) need to be machined to accommodate the dielectric strip, which further contributes to the mechanical tolerance problem. In this paper, we propose a new type of NRD-guide structure called the engraved NRD guide (ENRD), which could significantly alleviate the problem of alignment and mechanical tolerances, especially in the use of hybrid integrated planar NRD-guide technology. This new scheme of design was very briefly presented in [8], and it is made of a single dielectric block with a metal plate glued on one side for strength. By machining the dielectric block, only a necessary amount of dielectric material is removed from the block to form an equivalent NRD guide that has almost the same propagation constant. The remaining part of the dielectric block is kept in support of the cover, which could be a microstrip-line substrate (see Fig. 1). In this paper, electrical and mechanical properties of the ENRD guide will be studied and discussed for design considerations. With this new approach, a bandpass filter can be realized with a precision that only depends on that of the milling machine used. This approach could also ease the fabrication of a multicomponent NRD structure such as an ENRD-guide transceiver.

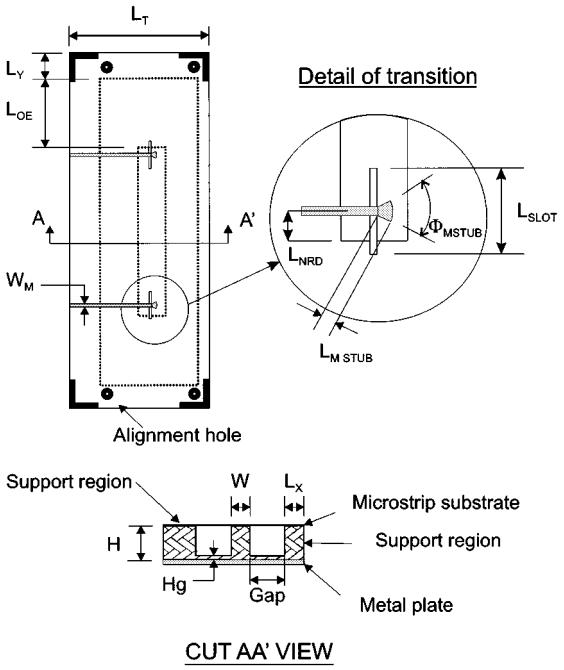

Fig. 1. Topology of an ENRD guide with two microstrip-to-ENRD-guide LSM_{10}-mode transitions.

II. Description of ENRD Guide

In a conventional NRD guide, a rectangular dielectric strip of height H and width W is placed between two parallel metallic

Manuscript received September 11, 2000. This work was supported by the Natural Sciences and Engineering Research Council of Canada.

The authors are with the Poly-Grames Research Center, Département de Génie Électrique, École Polytechnique de Montréal, Montréal, QC, Canada H3V 1A2 (e-mail: cassivy@grmes.polymtl.ca; deslad@grmes.polymtl.ca; wuke@grmes.polymtl.ca).

Publisher Item Identifier S 0018-9480(02)00744-5.

plates. The choice of the H value should respect the following criteria or design limitations for the nonradiating criteria:

$$\frac{\lambda_0}{2}\sqrt{\frac{1+\tan^2\left(k_{1e}\cdot\frac{W}{2}\right)}{1+\varepsilon_{r1}\tan^2\left(k_{1e}\cdot\frac{W}{2}\right)}} < H < \frac{\lambda_0}{2} \qquad (1)$$

in which λ_0 is the free-space wavelength, ε_{r1} is the relative dielectric constant of the material used for making the NRD guide, and k_{1e} is the transverse wavenumber of the TE_{10} even mode in the material [9]. The upper bound limit yields the maximum operable frequency of the NRD guide, while the lower bound limit implies that hybrid modes will emerge in the NRD guide. In an ENRD guide, the same limits should be respected even though the geometrical conditions are not necessarily the same. First, the ENRD guide may introduce a small vertical asymmetry that is nevertheless responsible for any potential leakage along the cross section. In addition, the cross section of the structure becomes an air/dielectric composite in which the air region or gap should be reduced to a certain minimum, thus limiting or slowing the decay of fields in the horizontal direction. This is quite different from the conventional NRD guide in which rapid field decay is observed immediately in the proximity of the air/NRD-strip interface. This suggests that an additional leakage is expected if the design is not made adequately. Therefore, the acceptable leakage level is used to determine the minimum air gap.

Fig. 1 illustrates the typical topology of an ENRD guide integrated with microstrip-to-NRD-guide transitions. It can be viewed as a leaky NRD waveguide, as described in [10], with the difference that dielectric slabs of width L_x are added on both sides of the guide, and that a certain amount of dielectric material of thickness Hg is left at the bottom of the guide. Due to that geometry, the ENRD guide have a complex leakage mechanism, which will be explained later.

The ENRD guide may be constructed in the following steps. First, a metal plate is glued to a dielectric block. Such a plate provides the strength needed for the machining step. The block is then machined to remove the necessary amount of dielectric material around the guide. A small thickness Hg of the dielectric material is left at the bottom of the air regions in order not to groove the metal plate. This is necessary because of a potential flatness problem of the metal plate. In practice, this thickness is smaller than 0.254 mm and could be reduced to 0.08 mm with good precision equipment. If the metal plate were to be grooved, it would leave a sharp metal edge that would produce a higher leakage level than by leaving a small amount of dielectric material of height Hg. Subsequently, alignment holes are made in the remaining part (support area) of the dielectric block. Finally, a microstrip substrate having the matching alignment holes is glued on top of the ENRD guide. This microstrip substrate is used to design millimeter-wave planar integrated circuits including LSM_{10}- or LSE_{10}-mode transitions or baluns of a microstrip-to-ENRD guide. The outcome of this process is a self-contained package that has repeatable performances due to its good alignment and mechanical tolerances.

III. Design of ENRD Guide

Even though the asymmetry of the ENRD guide may not lead to pure LSM_{10} or LSE_{10} modes [11], the principal modes of interest in the guide have propagation properties and field profile that are similar to those of a regular NRD guide. Therefore, we will continue to use the designation of LSM_{10} and LSE_{10} modes in this paper.

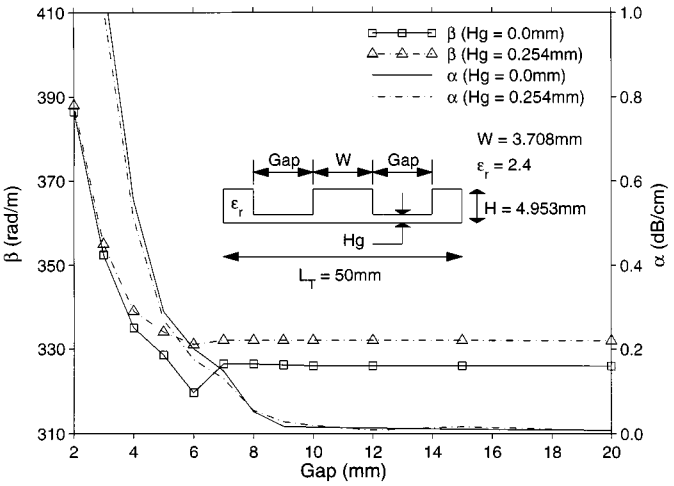

Fig. 2. Simulation results for the attenuation and phase constants of the LSM_{10} mode versus the gap size for $\varepsilon_r = 2.4$, $L_T = 50$ mm and frequency $= 28GHz$.

As for a regular NRD guide, the first step in the design of an ENRD guide is to determine the geometrical dimensions H and W for the frequency of interest and for the selected dielectric material. To do so, we make use of design curves presented in [4] for LSM_{10}-mode operation within an optimized frequency bandwidth.

The second step is the determination of the gap or air region width necessary on each side of the guiding dielectric strip. An adequate gap will yield a waveguide having almost the same propagation constant as a regular NRD guide, and also having an acceptable leakage level for both LSM_{10} and LSE_{10} modes. No special design software packages are currently available for this type of structure. To this end, a large number of simulations were carried out with a commercial three-dimensional (3-D) electromagnetic simulation software for dielectric material of $\varepsilon_r = 2.4$. Such efforts are to study effects of the gap on the propagation characteristics of the ENRD guide. Fig. 2 gives a set of simulation results for different gap size. A fixed width (L_T) of 50 mm is used for the complete structure. In our simulations, both bilateral sides of the structure are set to be radiating boundaries (or absorptive) and the dielectric loss is not taken into account. This is to help evaluating the field confinement in the guiding dielectric strip. The dimensions of the ENRD guide are selected to cover a frequency bandwidth of 26–30 GHz with a center frequency of 28 GHz.

Fig. 2 shows that the phase constant β of the LSM_{10} mode converges to a stable value while the attenuation constant α due to leakage becomes lower than 0.1 dB/cm as the gap is widen beyond 7.5 mm. For small gap value, the field cannot be decayed sufficiently in the gap region before going inside the support region where the condition stipulated in (1) is not respected, which produces a high leakage level. This situation is equivalent to the leaky NRD waveguide study in [10]. Fig. 2 also shows that a choice of Hg smaller than 0.254 mm has a negligible effect

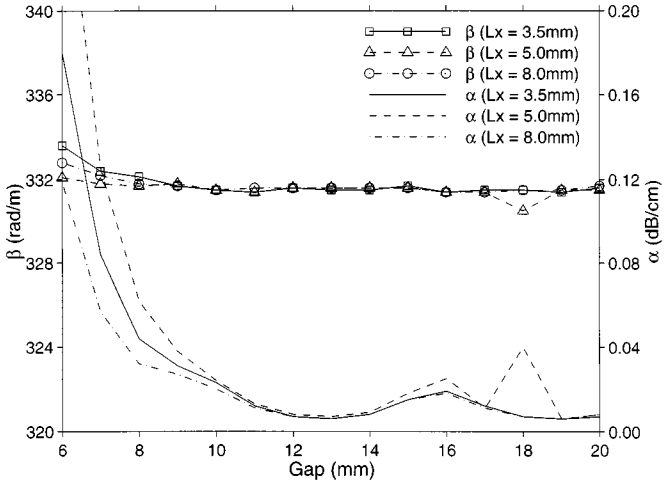

(a)

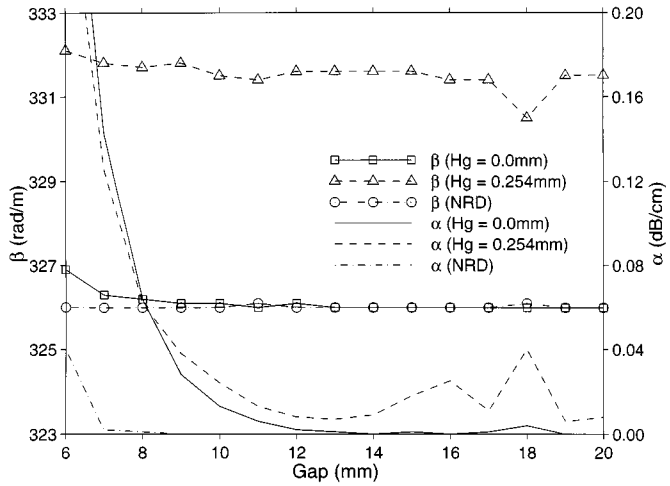

(b)

Fig. 3. Simulation results for the attenuation and phase constants of the LSM_{10} mode at 28 GHz versus the gap size with L_T variable. (a) Comparison of $L_x = 3.5$, 5.0, and 8.0 mm with $Hg = 0.254$ mm. (b) Comparison among the three cases: NRD guide, ENRD guide with $Hg = 0.254$ and $L_x = 5.0$ mm, and ENRD guide with $Hg = 0.0$ mm and $L_x = 5.0$ mm. For all the three structures, $\varepsilon_r = 2.4$, $H = 4.953$ mm and $W = 3.708$ mm.

on the propagation properties of the LSM_{10} modes because it causes a variation of β value less than 2%, and it has almost no effect on α.

In Fig. 3, the variation of β and α versus the gapwidth is presented with L_x made constant. In Fig. 3(a), comparison is made of the cases $L_x = 3.5$, 5.0, and 8.0 mm. It shows that the difference among the three cases for β is negligible (less than 1%). For α, however, the three values of L_x generate three different results. For a small gap (gap $<$ 10 mm), an L_x of 8.0 mm reduces the leakage level because the overall width of the guide (L_T) is the biggest among the three cases. However, the highest leakage level is obtained with an L_x of 5.0 mm. This is because this case produces a higher coupling with a "channel guide leaky mode," as described in [11]. This coupling also explains the difference of the three cases for the gap values of 16 and 18 mm.

In Fig. 3(b), the case of $L_x = 5.0$ mm is compared with another ENRD guide having the same dimension, except that $Hg = 0.0$ mm, and with an NRD guide having the same overall

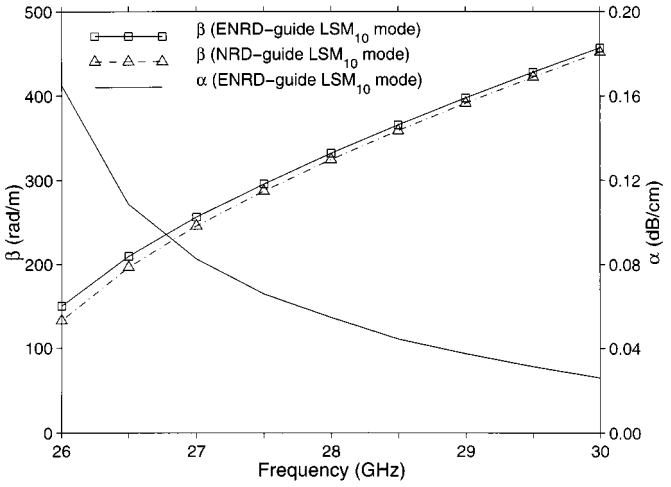

Fig. 4. Simulation results for the frequency variation of the phase and attenuation constants of the LSM_{10} mode in an ENRD guide of dimensions $H = 4.953$ mm, $W = 3.708$ mm, gap $= 8.0$ mm, $L_t = 50.0$ mm, and $\varepsilon_r = 2.4$. For comparison, the dispersion curve of an ideal NRD guide is added.

width as the other two guides. The results show that when $Hg = 0.0$ mm, β of the ENRD guide is equal to its corresponding NRD guide, except for the gap $<$8.0 mm. It also shows that when $Hg = 0.0$ mm, the leakage is reduced along with the coupling phenomena with the "channel guide leaky mode." This can be explained by the absence of asymmetry inside the ENRD guide when $Hg = 0.0$ mm, giving us a pure LSM_{10} mode with a field profile less compatible with the "channel guide leaky mode" [11]. Note that, for an NRD guide, the leakage is almost insignificant and no coupling phenomena are noticeable.

To examine frequency dependency of α and β, the gap and L_T are fixed at 8.0 and 50 mm, respectively. Dispersion curves are shown in Fig. 4 for the LSM_{10} mode, showing that dispersion characteristics of an ENRD guide are almost identical to those of a regular NRD guide. A minor difference can be seen for a slightly higher phase constant and a lower cutoff frequency for the LSM_{10} mode of the ENRD guide. On the other hand, the leakage is reduced with frequency. This suggests that the gapwidth should be determined at the lowest operating frequency if a specific maximum of α has to be observed over a frequency band of interest. The same scenario is also applicable to the LSE_{10} mode.

Before proceeding to a practical implementation of the ENRD-guide component, effects of the open-end spacing L_{OE} (see Fig. 1) should be discussed, which is important for the design of open ENRD guides in hybrid integration of planar and ENRD guide. Fig. 5 gives return loss S_{11} of an open ENRD guide in magnitude and phase for the LSM_{10} mode against L_{OE}. In the simulations, the gap is fixed at 8.0 mm with an ENRD guide of 10.5-mm long at $f = 28$ GHz, and no numerical deembedding is carried out. It can be seen that L_{OE} has little influence on S_{11} if it is longer than 11 mm. Simulation results for the LSE_{10} mode indicate the same behavior. Comparison of the open ENRD guide and its regular NRD-guide counterpart shows difference of 10° in-phase and 3.7% in magnitude for S_{11}. Such a difference is due to the

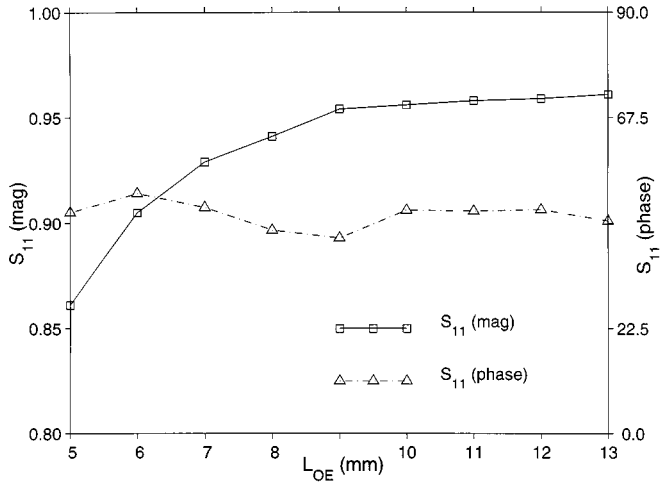

Fig. 5. Simulation results for S_{11} of an open-ended ENRD guide for the LSM_{10} mode versus L_{OE}, with $\varepsilon_r = 2.4$, gap $= 8.0$ mm, $H = .9534$ mm, $W = 3.708$ mm, and $L_y = 3.5$ mm at 28 GHz.

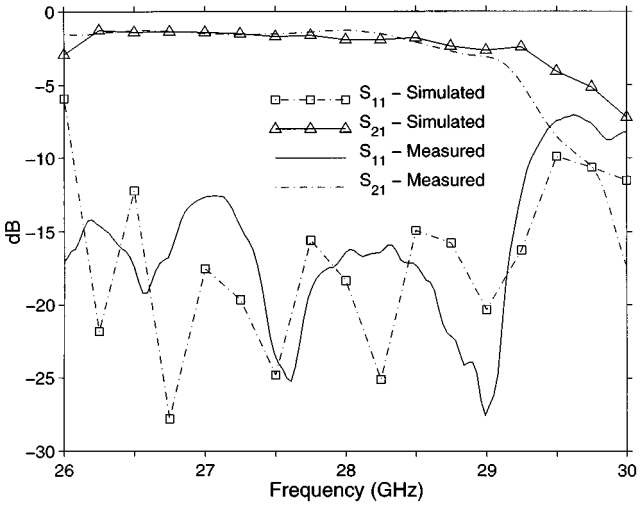

Fig. 6. Measured and simulated results for an ENRD guide with $\varepsilon_r = 2.4$, $H = 4.953$ mm, $W = 3.708$ mm, gap $= 7.26$ mm, and a length of 63.8 mm, excited using two identical back-to-back microstrip-to-ENRD-guide LSM_{10}-mode transitions.

higher phase constant and higher attenuation constant of the ENRD guide. The frequency dependency of both guides is similar.

Note that the preceding discussion is valid only for a dielectric material of $\varepsilon_r = 2.4$ (low dielectric constant). If another material with relatively higher dielectric constant is used, a further study should be carried out.

IV. Practical Examples of ENRD-Guide Component

A. Straight ENRD Guide

To validate our proposed concept of an ENRD guide, we constructed a straight ENRD guide with a gapwidth of 7.62 mm based on a dielectric material of $\varepsilon_r = 2.4$. The LSM_{10}-mode ENRD guide is sandwiched between two microstrip-to-ENRD-guide transitions [12], where the microstrip line is used for connecting the ENRD guide to an 8510C network analyzer. The length of the ENRD guide is 3.8 cm. Our experiments were made with an Anritsu SC5226 test fixture and a thru-reflect-line (TRL) calibration procedure. The geometrical dimensions of the whole structure (see Fig. 1) are $L_x = 3.5$ mm, $W = 3.71$ mm, $H = 4.95$ mm, gap $= 7.62$ mm, $Hg < 10$ mil, $L_T = 25.4$ mm, $L_{\mathrm{OE}} = 15$ mm, $L_{\mathrm{MSTUB}} = 0.99$ mm, $W_M = 0.61$ mm, $\Phi_{\mathrm{STUB}} = 50°$, $L_{\mathrm{slot}} = 6.1$ mm, and $L_{\mathrm{NRD}} = 2.464$ mm. The dielectric material used for the microstrip line is the RT/Duroid 5870 with $\varepsilon_r = 2.33$ and thickness $= 0.254$ mm. Measured and simulated results including dielectric loss are presented in Fig. 6, which show a good agreement between them.

Using the same ENRD-guide design platform, transmission performances of the structure are simulated and measured for LSE_{10}-mode transitions [13] of the microstrip-to-ENRD guide, as presented in Fig. 7. Once again, we observe a good agreement between them. Obviously, the LSM_{10}-mode results are better.

The above two examples have validated the concept of the ENRD guide. In the following, we will discuss some useful ENRD-guide discontinuities and their leakage effects in the design of ENRD-guide components.

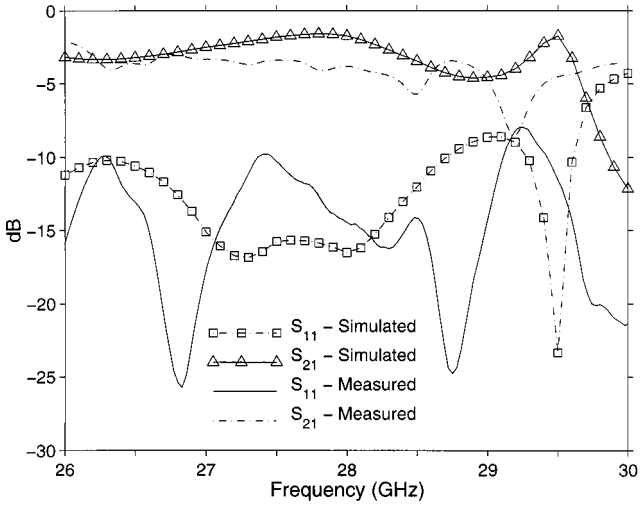

Fig. 7. Measured and simulated results for an ENRD guide with $\varepsilon_r = 2.4$, $H = 4.953$ mm, $W = 3.708$ mm, gap $= 7.26$ mm, and a length of 63.8 mm, excited using two identical back-to-back microstrip-to-ENRD-guide LSE_{10}-mode transitions.

B. 90° ENRD-Guide Bend

It is known that there is a mode conversion between the LSM_{10} and LSE_{10} modes in NRD-guide structures such as a T-junction or 90° bend [4], [14], [15]. This mode conversion cannot be eliminated without using a special measure like a mode suppressor. However, it can be optimized such that nearly all the power of the LSM_{10} mode at the input port is converted into the LSE_{10} modal power at the output port and vice versa. Using the design procedure described in [14], which gives an adequate dimension of 90° NRD-guide bend for optimum mode conversion, we constructed an ENRD-guide bend, as shown in Fig. 8(b), using a gap of 7.62 mm and a dielectric material with $\varepsilon_r = 2.4$.

Simulation results that do not include the dielectric loss are given in Fig. 9, which show an insertion loss of about 0.4 dB for the LSM-LSE mode conversion and a direct LSM-LSM mode

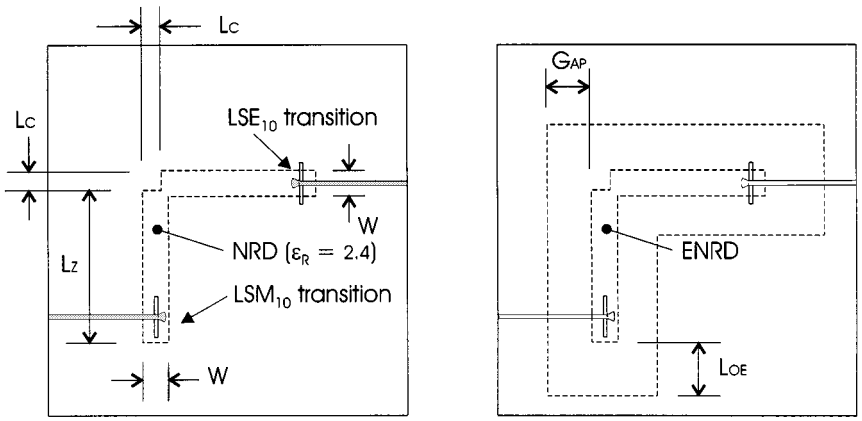

Fig. 8. Topology of: (a) NRD-guide 90° bend and (b) ENRD-guide 90° bend, both with two different microstrip-to-NRD-guide transitions for the mode conversion measurement.

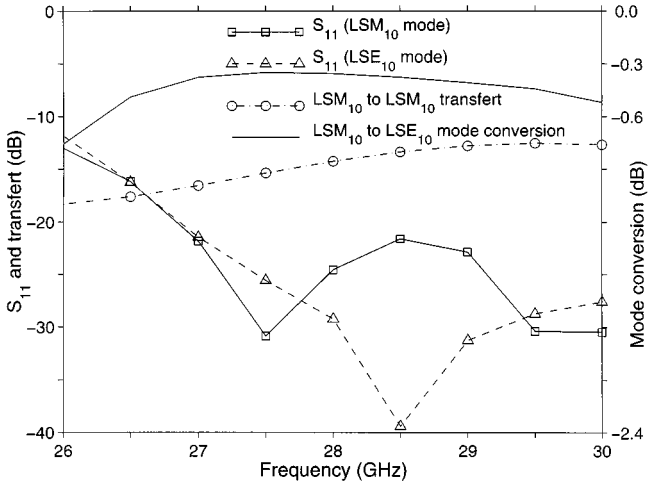

Fig. 9. Simulation results for an ENRD-guide 90° bend with $L_c = 2.781$ mm, $W = 3.708$ mm, $H = 4.953$ mm, and gap $= 7.62$ mm.

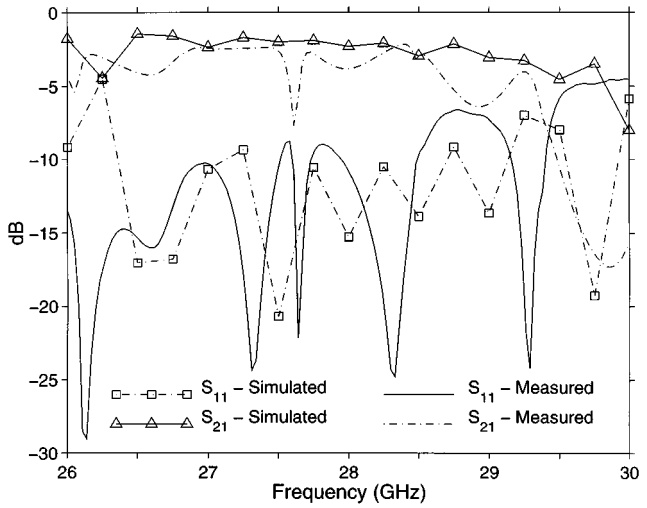

Fig. 10. Measured and simulated results for an ENRD-guide 90° bend with two back-to-back microstrip-to-ENRD-guide transitions; the first being an LSM_{10}-mode type and the second being an LSE_{10}-mode type.

transfer level below −12 dB. In the experiment, one port of the bend is excited by a microstrip-to-NRD-guide LSM_{10}-mode transition, while the other port of the device is connected to a microstrip-to-NRD-guide LSE_{10}-mode transition. This enables us to measure the mode conversion produced by the bend. Measured and simulated results that include the two transitions effects are presented in Fig. 10. If the insertion loss in the two transitions is taken into account, the LSM_{10} to LSE_{10} mode conversion loss is below 1 dB between 27.0–28.5 GHz, except at 27.6 GHz, where a notch is present. This notch is attributed to a resonance in the structure that reduces significantly the LSM_{10} to LSE_{10} mode conversion. It shows a good mode conversion with low leakage loss, even though the structure needs to be optimized.

C. ENRD-Guide Filter

Following the design rule developed in [4], an NRD-guide bandpass filter of third order is designed with a Polystyrene material $(\varepsilon_r = 2.4)$ of 4.953-mm thickness. The operating center frequency is 28 GHz and the bandwidth is 1.1%. Dimensions of the filter are summarized as follows (see Fig. 11): $L_1 = 4.954$ mm, $L_2 = 4.958$ mm, $S_1 = 3.763$ mm, and $S_2 = 7.989$ mm. The microstrip-to-ENRD-guide LSM_{10}-mode transitions used in this filter design are the same as in the previous examples.

The first filter prototype was built with a gap of 7.62 mm. Its insertion loss was measured to be 10 dB, which includes the filter loss as well as loss of the transitions (about 1.5 dB). This prohibitive insertion loss in the filter comes from the fact that, in this type of filter, each discontinuity or air gap between resonators generates a strong mode conversion between the guiding LSM_{10} mode in the ENRD guide and the evanescent LSM_{10} mode in the air gap. In the case of an NRD guide having infinitely extended metal plates, the evanescent LSM_{10} mode is fully characterized by a lossless attenuation constant $(\gamma = \alpha)$. This scenario is used in the design algorithm of the NRD-guide filter. However, in the case of finitely extended metal plates, the propagation constant γ of the evanescent LSM_{10} mode is defined by two constants β and α, where α is a combination of leakage loss and lossless attenuation. The leakage will increase the insertion loss of the filter. The phase constant will introduce a phase de-

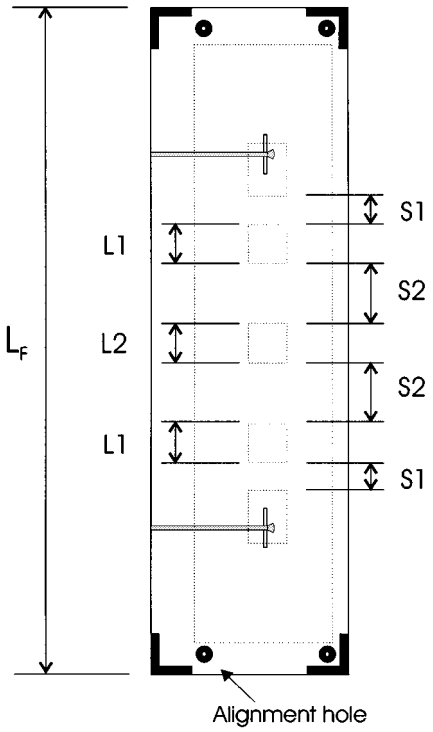

Fig. 11. Topology of the ENRD-guide bandpass filter with two identical back-to-back microstrip-to-ENRD-guide LSM_{10}-mode transitions.

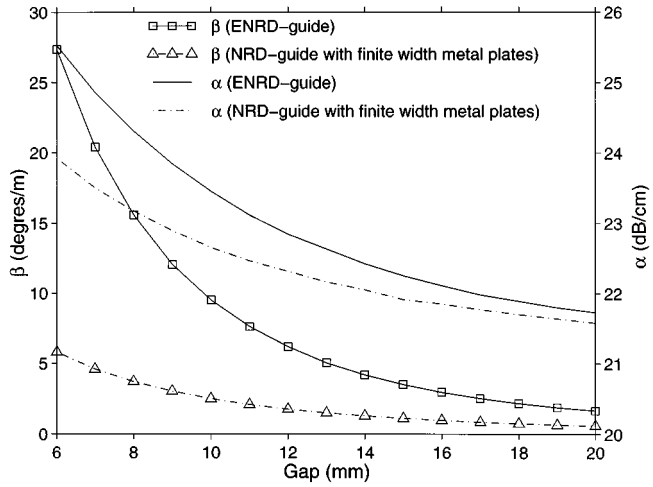

Fig. 12. Simulated results for the propagation characteristics of the LSM_{10} evanescent modes of a NRD guide (with finite metal plate width) and an ENRD guide versus gap value with $L_x = 3.5$ mm at 28 GHz.

viation from the desired level of design between the resonators that will alter the shape of frequency response of the filter.

In an ENRD guide, the α and β constants of the evanescent mode depend on the choice of the gap and width L_x. Due to a weak confinement of the fields, this mode has a higher leakage than the guiding LSM_{10} mode. Fig. 12 gives calculated propagation characteristics of the evanescent LSM_{10} mode for both the NRD guide with finite-width metal plates and the ENRD guide, showing that the ENRD-guide filter has a higher loss and phase variation than its NRD-guide counterpart having the same metal plate width. It also suggests that we should substantially increase the gapwidth to reduce the insertion loss

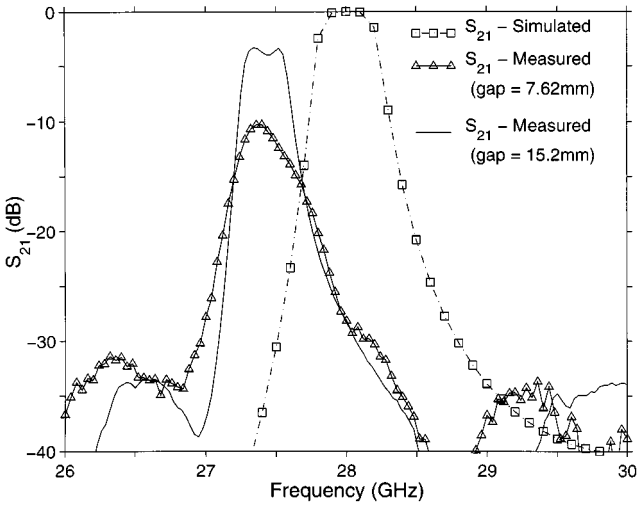

Fig. 13. Simulated and measured results for ENRD-guide bandpass filters.

level. By widening the gap to 15.2 mm, we are able to reduce the loss by 2.4 dB/cm, as compared to the previously designed ENRD-guide filter. This corresponds to a reduction of 5.64 dB for the insertion loss, considering that the length of air gap is 2.35 cm in the filter. Fig. 13 presents measured results of two ENRD-guide filters, one with a gap of 7.62 mm and the other with a gap of 15.2 mm. Indeed, we can observe a remarkable improvement (more than 5.6 dB) in the passband of the filter. For a further improvement, a low-loss dielectric material has to be used instead of our Polystyrene material that has a less favorable loss tangent (0.002). In addition, the results also indicate that, the higher phase constant of the evanescent LSM_{10} mode, in the case of a gap of 7.62 mm, noticeably degrades the shape of the filtering response.

Finally, we should mention that a difference of 600 MHz between the center frequency of the simulated filter and the center frequency of the measured filters may be caused by the mechanical tolerance of the build circuit, especially the height (H), and the tolerance on the relative dielectric constant of the material.

V. Conclusions

In this paper, we have presented a new design platform of an NRD guide, called the ENRD guide, for the construction of millimeter-wave integrated circuits. Design considerations and parametric influences of the proposed structure are studied and discussed with respect to its practical implementation. The design guidelines are established, indicating that a low-leakage loss level is achievable if extra care is taken in the determination of the gap size and width L_x of the guide. Practical realization of an ENRD guide shows a good and predictable performance, especially when transitions of the microstrip-to-ENRD guide are used. On the other hand, the measured results of a 90° ENRD-guide bend suggest that a strong mode conversion between the LSM_{10} and LSE_{10} modes is possible. Also, it is shown that, for the ENRD-guide resonator filters, the gap should be large enough so to prevent a prohibitive insertion loss caused by the leakage of the evanescent LSM_{10} mode existing between the resonators. Design curves for the selection of the appropriate gap size are presented.

The new NRD-guide structure is believed to ease the integration of multiple NRD-guide components, thus paving the way of constructing a low-loss hybrid integrated planar NRD transceiver.

ACKNOWLEDGMENT

The authors would like to thank J. Gauthier, Poly-Grames Research Center, École Polytechnique of Montréal, Montréal, QC, Canada, for his help in this work.

REFERENCES

[1] T. Yoneyama and S. Nishida, "Nonradiative dielectric waveguide for millimeter-wave integrated circuits," *IEEE Trans. Microwave Theory Tech.*, vol. MTT-29, pp. 1188–1192, Nov. 1981.

[2] J. A. G. Malherbes, "Radiation from a wedge-type nonradiative dielectric waveguide radiator," *Microwave Opt. Technol. Lett.*, vol. 21, pp. 313–315, June 1999.

[3] T. Yoneyama, F. Kuroki, and S. Nishida, "Design of nonradiative dielectric waveguide filters," *IEEE Trans. Microwave Theory Tech.*, vol. MTT-32, pp. 1622–1659, Dec. 1984.

[4] F. Boone and K. Wu, "Mode conversion and design consideration of integrated nonradiative dielectric (NRD) components and discontinuities," *IEEE Trans. Microwave Theory Tech.*, vol. 48, pp. 482–492, Apr. 2000.

[5] K. Wu and L. Han, "Hybrid integrated technology of planar circuits and NRD-guide for cost-effective microwave and millimeter-wave applications," *IEEE Trans. Microwave Theory Tech.*, vol. 45, pp. 946–954, June 1997.

[6] W. X. Zhang and L. Zhu, "New leaky-wave antenna for millimeter waves constructed from groove NRD waveguide," *Electron. Lett.*, vol. 23, pp. 1191–1192, Oct. 1987.

[7] Z. Ma and E. Yamashita, "Wave leakage from groove NRD structures," *IEEE Microwave Guided Wave Lett.*, vol. 3, pp. 170–172, June 1993.

[8] Y. Cassivi, D. Deslandes, and K. Wu, "Engraved NRD-guide for millimeter-wave integrated circuits," in *IEEE MTT-S Int. Microwave Symp. Dig.*, Boston, MA, 2000, pp. 605–608.

[9] M. Cohn, "Propagation in a dielectric-loaded parallel plane waveguide," *IRE Trans. Microwave Theory Tech.*, vol. MTT-8, pp. 202–208, Apr. 1959.

[10] A. Sanchez and A. A. Oliner, "A new leaky waveguide for millimeter waves using nonradiative dielectric (NRD) waveguide—Part I: Accurate theory," *IEEE Trans. Microwave Theory Tech.*, vol. MTT-35, pp. 737–747, Aug. 1987.

[11] H. Shigesawa, M. Tsuji, and A. A. Oliner, "Effects of air gap and finite metal plate width on NRD guide," in *IEEE MTT-S Int. Microwave Symp. Dig.*, 1986, pp. 119–122.

[12] Bacha and K. Wu, "Toward an optimum design of NRD-guide and microstrip-line transition for hybrid-integrated technology," *IEEE Trans. Microwave Theory Tech.*, vol. 46, pp. 1796–1800, Nov. 1998.

[13] A. Bacha and K. Wu, "LSE-Mode balun for hybrid integration of NRD-guide and microstrip line," *IEEE Microwave Guided Wave Lett.*, vol. 8, pp. 199–201, May 1998.

[14] F. Boone, "Étude et conception de composants passifs en technologie NRD pour applications en ondes millimétriques," Ph.D. dissertation, Dept. Elect. Eng., École Polytech. Montréal, Montréal, QC, Canada, 2000.

[15] Y. Endo and T. Yoneyama, "Finite element analysis of discontinuities in nonradiative dielectric waveguide," *Electron. Commun. Japan*, pt. 2, vol. 72, pp. 102–112, Nov. 1989.

Yves Cassivi was born in New-Richmond, QC, Canada. He received the Eng. Dipl. degree in electrical engineering and the Masters degree in applied science from the École Polytechnique de Montréal, Montréal, QC, Canada, in 1989 and 1991, respectively, and is currently working toward the Ph.D. degree at the Poly-Grames Research Center, Département de Génie Électrique, École Polytechnique de Montréal, Montréal, QC, Canada.

From 1993 to 1995, he was a Professor at the Collège d'Enseignement Général et Professionnel de la Gaspésie et des Iles, Gaspé, QC, Canada. From 1996 to 1999, he was with SR Telecom Inc., Montréal, QC, Canada, where he was a RF/Microwave Designer.

Dominic Deslandes was born in Drummondville, QC, Canada, in 1975. He received the Eng. Dipl. degree in electrical engineering from the Université de Sherbrooke, Sherbrooke, QC, Canada, in 1998, and is currently working toward the M.S. degree in microwaves at the École Polytechnique de Montréal, Montréal, QC, Canada.

His current research interests include design of passive and active millimeter-wave components.

Ke Wu (M'87–SM'92–F'01) was born in Liyang, Jiangsu Province, China. He received the B.Sc. degree in radio engineering (with distinction) from the Nanjing Institute of Technology (now Southeast University), Nanjing, China, in 1982, and the D.E.A. and Ph.D. degrees in optics, optoelectronics, and microwave engineering (with distinction) from the Institut National Polytechnique de Grenoble (INPG), Grenoble, France, in 1984 and 1987, respectively.

He conducted research in the Laboratoire d'Electromagnetisme, Microondes et Optoelectronics (LEMO), Grenoble, France, prior to joining the Department of Electrical and Computer Engineering, University of Victoria, Victoria, BC, Canada. He subsequently joined the Department of Electrical and Computer Engineering, École Polytechnique de Montréal, Montréal, QC, Canada, as an Assistant Professor, and is currently a Full Professor. He has held visiting or guest professorships at Telecom-Paris, Paris, France, and INP-Grenoble, Grenoble, France, the City University of Hong Kong, the Swiss Federal Institute of Technology (ETH-Zurich), Zurich, Switzerland, the National University of Singapore, Singapore, the University of Ulm, Ulm, Germany, as well as many short-term visiting professorships at other universities. He also holds an Honorary Visiting Professorship at the Southeast University, China. He has been the Head of the FCAR Research Group of Quebec on RF and microwave electronics, and the Director of the Poly-Grames Research Center, as well as the Founding Director of the newly developed Canadian Facility for Advanced Millimeter-wave Engineering (FAME). He has authored or co-authored over 300 referred journal and conference papers, and also several book chapters. His current research interests involve three-dimensional (3-D) hybrid/monolithic planar and nonplanar integration techniques, active and passive circuits, antenna arrays, advanced field-theory-based computer-aided design (CAD) and modeling techniques, and development of low-cost RF and millimeter-wave transceivers. He is also interested in the modeling and design of microwave photonic circuits and systems. He is an Editorial Board member for *Microwave and Optical Technology Letters*.

Dr. Wu is a member of the Electromagnetics Academy. He was chairperson of the 1996 Symposium on Antenna Technology and Applied Electromagnetics (ANTEM) Publicity Committee and vice-chairperson of the Technical Program Committee (TPC) for the 1997 Asia–Pacific Microwave Conference (APMC'97). He has served on the FCAR Grant Selection Committee and the TPC committee for the International Conference on Telecommunications in Modern Satellite Cable and Broadcasting Services (TELSIKS) and International Microwave and Optical Technology (ISMOT). He has also served on the ISMOT International Advisory Committee. He was the general co-chair of the 1999 and 2000 SPIE International Symposium on Terahertz and Gigahertz Electronics and Photonics, Denver, CO, and San Diego, CA, respectively. He was the general chair of the 8th International Microwave and Optical Technology (ISMOT'2001), Montreál, QC, Canada, June 19–23, 2001. He has served on the Editorial or Review Boards of various technical journals, including the IEEE TRANSACTIONS ON MICROWAVE THEORY AND TECHNIQUES, the IEEE TRANSACTIONS ON ANTENNAS AND PROPAGATION, and the IEEE MICROWAVE AND GUIDED WAVE LETTERS He served on the 1996 IEEE Admission and Advancement (A&A) Committee, the Steering Committee for the 1997 joint IEEE Antennas and Propagation Society (IEEE AP-S)/URSI International Symposium. He has also served as a TPC member for the IEEE Microwave Theory and Techniques Society (IEEE MTT-S) International Microwave Symposium. He was elected to the Board of Directors of the Canadian Institute for Telecommunication Research (CITR). He also serves on the Technical Advisory Board of Lumenon Lightwave Technology Inc. He is currently the chair of the joint IEEE chapters of the IEEE MTT-S/IEEE AP-S/IEEE Lasers and Electro-Optics Society (IEEE LEOS), Montreál, QC, Canada. He was the recipient of the URSI Young Scientist Award, the Institute of Electrical Engineers (IEE), U.K., Oliver Lodge Premium Award, the Asia–Pacific Microwave Prize Award, the University Research Award "Prix Poly 1873 pour l'Excellence en Recherche" presented by the École Polytechnique on the occasion of its 125th anniversary, and the Urgel–Archambault Prize (the highest honor) in the field of physical sciences, mathematics and engineering presented by the French–Canadian Association for the Advancement of Science (ACFAS).